The impacts of different PBL schemes on the simulation of $PM_{2.5}$ during severe haze episodes in and surrounding the Jing-Jin-Ji region, China

Tian Li [1], Hong Wang[2], Tianliang Zhao [1], Min Xue[2], Yaqiang Wang [2], Huizheng Che [2], Chao Jiang [3]

1 Collaborative Innovation Center on Forecast and Evaluation of Meteorological Disasters, Key Laboratory for Aerosol-Cloud-Precipitation of China Meteorological Administration, Nanjing University of Information Science and Technology, Nanjing 210044, China

2 State Key Laboratory of Severe Weather/Institute of Atmospheric Composition, Chinese Academy of Meteorological Sciences (CAMS), CMA, Beijing 100081, China

3 Yantai Meteorological Bureau, Yantai 264003, China

Correspondence to: Li Tian (njlitian@126.com) and Wang Hong **(**wangh@cams.cma.gov.cn**)**

Abstract

To explore the impacts of different PBL schemes on the simulation of high $PM_{2.5}$ concentrations during severe haze in China, four schemes [Yonsei University (YSU), Mellor-Yamada-Janjic (MYJ), Asymmetric Convection Model, version 2 (ACM2), and Bougeault–Lacarrère (Boulac)] were employed in the Weather Research and Forecasting/Chemistry (WRF-Chem) model to simulate the severe haze that occurred in February 2014 in and surrounding the Jing-Jin-Ji region—one of China's most polluted regions in recent years. The $PM_{2.5}$ concentration simulated using the four schemes, together with the meteorological factors closely related to $PM_{2.5}$ (wind speed, local vertical diffusion and PBL height), were evaluated through comparison with observations. The simulated results of stations in different terrains were also compared with observations. The results indicated that the eastern plain cities produced better simulation results than the western cities, and the cities under the eastern root of Taihang Mountain produced the worst results in simulating high PM2.5 concentration in haze. All four schemes simulated very similar daily variation of the surface $PM_{2.5}$ concentration compared with observations from 1 to 28 February, 2014. The Boulac scheme was found to be the best among the schemes in terms of its representation of the polluted period, followed by the YSU and MYJ scheme. Owing to its absence of diffusivity in the chemistry module, the surface $PM_{2.5}$ concentration simulated using the ACM2 scheme was obviously higher than observed, as well as compared with the three other PBL schemes. The diurnal variations of surface $PM_{2.5}$ simulated using the four schemes were not as reasonable as their reflection of daily averaged variation. The simulated concentrations of surface $PM_{2.5}$ using the YSU, MYJ and Boulac schemes all showed large negative errors during daytime on polluted days due to their inefficient descriptions of strong local atmospheric stability or extremely weak diffusivity processes under severe haze pollution in Jing-Jin-Ji region. The lower ability of PBL schemes in distinguishing the local PBL meteorologies including daytime diffusion and wind speed between haze and clean days in the complex topography area in China is a main problem for PM2.5 forecasting, which is worthy of being studied in detail. This also should be noted when the WRF-Chem model is used to simulate and study severe haze pollution in China.

Keywords: $PM_{2.5}$ simulation, PBL scheme, haze episode, vertical diffusivity, PBL height

1.Introduction

Owing to its population explosion, accelerated urbanization, and globalization, China—the country with the fastest growing economy in the world—has been suffering from increasingly severe air pollution since the 1980s. Related to this, haze occurrence in China, on the whole, has continued to grow during the past several decades, especially after 1980 [1]. Today, haze is a frequent phenomenon in most areas of eastern China, leading to adverse economic as well as human health impacts [2]. Broadly, four severe haze regions in China are recognized: Beijing, Tianjin, Hebei Province (abbreviated to Jing-Jin-Ji) and its surroundings [3-5]; the Yangtze River Delta; Pearl River Delta; and the Sichuan Basin. As one of the most important unban agglomerations in China, the Jing-Jin-Ji region and its surroundings has attracted considerable attention recently, because of the serious pollution episodes it has experienced since 2013. Multi-source observations that can characterize the haze process in Jin-Jin-Ji and its surrounding areas have been used to study the temporal and spatial variation of haze, meteorological conditions, and the chemical components of haze [6-12]. Based on these extensive observational studies, continuous studies of the resultant pollution emissions inventory have also been conducted [13-15]. In addition, a number of simulation studies using atmospheric models have been carried out to study haze and pollutions processes in China; these studies involve the interactions between meteorological conditions, particle concentrations, and the variation in the transport characteristics of pollutants during the pollution process [16-20]. There are two key factors involved in the formation and persistence of haze: one is fine particulate matter ($PM_{2.5}$) and gas pollutants (O_3, SO_2, NOx, etc.), and the other is meteorological conditions. Moreover, when modeling haze, there are uncertainties related to the planetary boundary layer (PBL), which mainly derive from the particular PBL scheme used; and therein, the PBL height (PBLH), turbulent mixing process, and wind fields are major variables controlling the haze process in the PBL [21-23]. Therefore, the PBL scheme is a vital factor of influence in terms of modeling the formation and maintenance of haze and air pollution [24, 25]. A lower PBLH and weaker PBL turbulence diffusion are regarded as key meteorological aspects for haze formation [26]. Studies on different PBL parameterization schemes have shown that an accurate depiction of the meteorological conditions within the PBL via an appropriate PBL parameterization scheme is important for air pollution modeling [27-29]. Some studies have also discussed the importance of the PBL scheme in the modeling of O_3 concentrations; specifically, in the U.S.A and using Weather Research and Forecasting/Chemistry model (WRF-Chem) [30-32]. These studies also touched upon the possible effects of the PBL scheme on the modeling of $PM_{2.5}$; however, little is known about whether current PBL schemes are efficient in modeling extremely high $PM_{2.5}$ concentrations and haze events over the Chinese mainland.

In order to investigate the abilities of PBL schemes in modeling $PM_{2.5}$ over the Jing-Jin-Ji region during serious haze events with high $PM_{2.5}$ values, and to provide instructive guidance regarding $PM_{2.5}$ prediction over this region, separate WRF-Chem model simulations using four popular PBL schemes [Yonsei University (YSU), Mellor-Yamada-Janjic (MYJ), Asymmetric Convection Model, version 2 (ACM2), and Bougeault–Lacarrère (Boulac)] were run for haze episodes that occurred in February 2014. After first introducing the methodolody, model configuration and data used, we then evaluate the $PM_{2.5}$ simulation results from the four PBL schemes by comparing with observations, as well as analyze the related meteorological fields. Finally, conclusions are drawn regarding the impacts of the PBL on $PM_{2.5}$ simulation, along with a discussion on the possible underlying physical mechanisms involved.

2. Methodolody

2.1 Model Introduction and Configureation

The WRF-Chem model is a fully coupled "online" model, with its air quality component fully consistent with the meteorological component [33, 34]. Version 3.5 of WRF-Chem was employed in this study. Two nested domains (Fig. 1) were used in the simulation with grid spacing of 27 km and 9 km, respectively. The inner domain was centered at (115°E, 35.5°N) on a Lambert map projection. Considering the regional transmission of $PM_{2.5}$ during haze processes, the main research area of domain 2 ranged over (111°E–120.5°E, 34.5°N–42.5°N), containing the whole Jing-Jin-Ji area and its upstream region including most areas of Shanxi and Shandong provinces and part of Henan Province—both regarded as contributors to Jing-Jin-Ji's pollution. The research area is abbreviated as 3JNS hereafter. The two domains used the same 35 vertical levels extending from the surface to 10 hPa, and the layer heights within PBL are showed in Table 3. The simulation period ranged from 00:00 UTC January 28, 2014 to 00:00 UTC March 1, 2014. The simulation outputs from February 1 to 28 were used to obtain the chemical component balance from pollutant emissions.

The CBM-Z chemistry mechanism [35] combined with MADE/SORGAM (Modal Aerosol Dynamics Model for Europe and Secondary Organic Aerosol Model) was applied in each domain, and the Fast-J photolysis scheme [36] coupled with hydrometeors, aerosols and convective parameterizations was chosen. All domains used the RRTM scheme [37] for longwave radiation, the Goddard scheme for shortwave radiation, the Lin (Purdue) microphysics scheme [38], and the New Grell scheme for cumulus parameterization (Table 1). Four PBL schemes—YSU, MYJ, ACM2, and Boulac—were adopted in the model runs.

2.2 Emissions Intruction

The anthropogenic emissions of chemical species, with resolution of 0.1° × 0.1°, came from the Multi-resolution Emissions Inventory for China (MEIC) for 2010 (http://www.meicmodel.org), which was developed in 2006 for the INTEX-B mission[13]. The inventory includes 10 major kinds of pollutants and greenhouse gases and more than 700 kinds of anthropogenic emissions, which can be divided into five sources: transportation, residential, industry, power, and agricultural. According to the INTEX-B inventory, the main pollutants in China that year were SO_2, NOx, CO, NMVOC, PM_{10}, $PM_{2.5}$, BC, and OC. This 2010 emissions inventory has been validated as credible and widely used in studies of pollution in China [14, 15, 39].

2.3 Data Descriptions

The National Centers for Environmental Prediction (NCEP) reanalysis data (resolution: 1°×1°) were used for the model's initial and boundary conditions. The hourly surface $PM_{2.5}$ observational data for February 2014 from the China National Environmental Monitoring Center were used to evaluate the model results. There are 109 $PM_{2.5}$ sites in domain 2 and 48 sites in 3JNS. The results presented in this paper focus mainly on the sites (evenly distributed) in 3JNS. Surface and vertical sounding balloon observations of the Meteorological Information Comprehensive Analysis and Process System (MICAPS) from the China Meteorological Administration were also used for evaluating and analyzing the model. The locations of all these observational sites in domain 2 are marked in Figure 1. There are 88 MICAPS stations in 3JNS.

In order to explore the PBL schemes performance in different area, five stations—Beijing (under the Yan Mountain), Taiyuan (on the west side of Taihang Mountain), Zhangjiakou (in the northwest of 3JNS), Cangzhou (the coastal station), and Xingtai (the east foot of Taihang Mountain) were picked up to represent five topography and surface type in the 3JNS. The location of their abbreviations are displayed in the Figure 1.

2.4 PBL schemes Introduction

PBL schemes can be classified as local or nonlocal closure schemes [40], with the former obtaining the turbulent fluxes of each grid from mean variables, and the latter by considering the grid and its surroundings. Additionally, nonlocal schemes are able to simulate the fluxes and profiles of the convective boundary layer. The YSU PBL scheme—an improved version of the Medium-Range Forecast (MRF) scheme, with a critical bulk Richardson number of 0.25 over land—is a revised vertical diffusion package with a nonlocal coefficient in the PBL. Compared with the MRF scheme, it increases boundary layer mixing in the thermally induced free convection regime and decreases it in the mechanically induced forced convection regime. In addition, this scheme is also a relatively mature scheme that is able to simulate a realistic structure of the PBL in the WRF model [41, 42]. The MYJ PBL scheme is a turbulent kinetic energy (TKE) local closure scheme that defines the eddy diffusion coefficients by forecasting the TKE. This scheme is suitable for all stable and weakly unstable boundary layers [43]. The ACM2 PBL scheme features nonlocal upward mixing and local downward mixing. Compared with ACM1, it incorporates local turbulent transport and is able to simulate realistic vertical parameter profiles of the PBL [44]. However, the turbulent diffusion coefficient of ACM2 is not diagnosed in the chemical module (default value of 1E-06) [32]; thus, ACM2 is used as a reference scheme for comparing with the other three schemes in detail later in the paper. The Boulac scheme, regarded as a local closure scheme, has long been regarded as satisfactory in terms of its performance in orography-induced events[45]. These four PBL schemes are widely used in meso-scale or weather-scale modeling, and their respective merits and/or shortcomings have been reported in previous studies. They were also selected for use in the present reported study.

3. Results and discussion

3.1 Evaluation of surface $PM_{2.5}$

To validate the efficiencies of the four PBL schemes in simulating $PM_{2.5}$ in the Jing-Jin-Ji region, the spatial distribution of the modeled $PM_{2.5}$ values are compared with observations for a severe and long-lasting haze episode in this region. Figure 2 displays the averaged $PM_{2.5}$ distribution from 00:00 UTC February 21 to 00:00 UTC February 25, together with the observed values during the same period. The period-averaged $PM_{2.5}$ values reached 300–500 μg m^{-3} at observation sites over this region (marked with dots in Figure 2), and the instantaneous values were even higher; the $PM_{2.5}$ concertration in some cities (e.g., Beijing, Xingtai and Tangshan) even reached above 500 μg m^{-3} (Figure 3). Furthermore, as shown in Figure 2 and Figure 3, cities in southern Heibei Province endured more severe pollution than northern areas (e.g., Chengde, Zhangjiakou). For this haze period, the model results using the four PBL schemes were all reasonable; the observed and simulated distributions of $PM_{2.5}$ showed reasonable consistency. The differences in distributions between the YSU, MYJ and Boulac schemes were small, but the simulation values using the ACM2 scheme were obviously higher than observed. To evaluate the accuracies of the four PBL schemes in modeling the the variation in $PM_{2.5}$, 10 representative cities in 3JNS were selected (locations displayed in Figure 2), and their hourly variations in $PM_{2.5}$ concentration, as modeled using the four PBL schemes, were compared with observations for the period from 00:00 UTC February 1 to 00:00 UTC March 1 (Figure 3). The results show that all four PBL schemes produced similar representations of the real variation in $PM_{2.5}$ for the whole of Feburary. As the concentration of PM2.5 is the primary indicators in haze periods, so it can be seen from the Figure 3 that there were two main haze events in Feberary: one from February 13 to 15, and the other from February 21 to 25. The start and end points of these two events were each modeled well using the four PBL schemes. However, as the simulated conditions of the second event (February 21 to 25) were more accurate, this one was chosen as the research period in this study. In terms of the simulations at individual stations, eastern cities (e.g., Hengshui, Cangzhou and Chengde) produced better simulation results than western cities (e.g., Zhangjiakou, Baoding) for this event overall, suggesting that the PBL schemes possess properties that are more suited to simulating the $PM_{2.5}$ concentration in particular localities/regions. As for how model behaves for particular localities (plains, mountains, or coastal areas, etc.) by using these 4 PBL schemes, we will discuss about this later. There was little difference in the variation of $PM_{2.5}$ when using the YSU, MYJ and Boulac schemes, while the results of ACM2 were obviously higher than those of the other three schemes—attributable to the fact that the turbulent diffusion was not calculated in the chemistry module.

Four statistical indicators [mean bias (MB), normalized mean bias (NMB), normalized mean error (NME), and root mean square error (RMSE)] of the haze episode, clean days, and whole month averaged over 3JNS were calculated to evaluate the abilities of the four PBL schemes in simulating $PM_{2.5}$ (Table 2). The mean and extreme values of haze and clean periods using each PBL scheme, except ACM2, are also displayed in Table 2. The results show that the $PM_{2.5}$ modeled during the haze episode was better than that for the whole month. NB and NMB values of less than zero indicate the model results were an underestimation of the actual situation. The YSU, MYJ and Boulac schemes underestimated the $PM_{2.5}$ concentration during daytime but overestimated it at night, the reason for which will be discussed later in the paper. The Boulac scheme produced the least bias for haze episode compared with the other three schemes, followed by the YSU scheme, MYJ scheme, and finally the ACM2 scheme. The MB, NMB, NME and RMSE values further illustrate that the YSU, MYJ and Boulac schemes differed little in terms of their simulation of the $PM_{2.5}$ concentration during haze. The simulated values produced by ACM2, however, were much higher than those of the other three schemes.

3.2 Relationship between PBL meteorology and $PM_{2.5}$

The daily averaged values of $PM_{2.5}$ concentration, surface wind speed, PBLH, and vertical diffusivity at level 8 (Table 3) in 3JNS for the whole of Feburary are showed in Figure 4. The $PM_{2.5}$ values were determined by averaging the $PM_{2.5}$ data of 48 observation stations (Figure 1), and the wind speed values were the average of data of 88 CMA surface monitoring stations in the same area. The four PBL schemes all showed similar trends as those observed. As indicated by the results in Figure 4, the $PM_{2.5}$ modeled using the YSU, MYJ and Boulac schemes showed very little difference. The ACM2 scheme, however, simulated higher $PM_{2.5}$ than ovserved throughout almost the entire month, while its daily variation was comparable with the other three schemes. The four schemes all simulated similar daily trends for surface wind speed, which were in agreement with the observed trend, though they were all higher than observed. All four schemes showed the $PM_{2.5}$ concentration to possess an accurate inverse relationship with wind speed in terms of the daily averaged variation trend. The daily variation in $PM_{2.5}$ concentration also possessed a good inverse relationship with the PBLH (averaged over 48 sites, same for vertical diffusion), but not as obviously as that between $PM_{2.5}$ and surface wind speed. This suggested that a lower PBLH is an essential prerequisite for haze episodes; but when the PBLH is lower than a certain value, such as 400 m, its relationship with $PM_{2.5}$ is not so close. Considering their different diagnoses, the specific values between different PBL schemes are not comparable, so the focus here is their relationship with PM2.5, wind speed and vertical diffusivity. The anti-correlation between the daily $PM_{2.5}$ and vertical diffusivity of the YSU, MYJ and Boulac schemes was even weaker than that between $PM_{2.5}$ and the PBLH, indicating that the impact of local vertical diffusivity on the time scale of the daily averaged change trend of $PM_{2.5}$ is limited. Nevertheless, its impact on the hourly change of $PM_{2.5}$ during the daytime is clearer and more important, which will be disscussed in the section 3.4.

To illustrate the modeling performance by using four PBL schemes in different topographies, Figure 5 displays the simulated and observed daily averaged PM2.5 concentration and wind speed in the whole Feburary of five stations which can represent five topographies in the 3JNS (Figure 1). It can be seen from the figure that PBL schemes can depict appropriate variation trends compared with observation as to PM2.5 concentrations and wind speed, and they showed a good negative correlation with each other. The difference of PM2.5 concentration in YSU, MYJ, and Boulac schemes are still little in seperate stations, and the results by ACM2 schemes are apparently higher than the other three schemes. Meanwhile, the modeling results in different terrian contain certain differences. In this haze process, the modeling PM2.5 concentrations in some stations are slightly higher than the observations (Beijing, Taiyuan), while some are lower (Zhangjiakou, Xingtai), and the eastern coastal city (Cangzhou) performed well in this simulation. It is worth mentioning that the Xingtai station, representing the eastern foot of Taihang Mountain, has obviously lower simulating PM2.5 concentration than the observation by the four schemes, which can be mainly owing to the extremely higher simulation of wind speed (Fig. 5). Compared with near stations on the eastern Taihang Mountain, it can be found that Shijiazhuang and Handan also have the similar phenomena (lower simulated PM2.5 and higher simulated wind speed). It should be noted here that the higher simulated wind speed is one main but probably not the only reason contributing to the higher simulated PM2.5. In conclusion, the performance of schemes in the eastern root of Taihang Mountain, the most polluted region by haze in China, were relatively poor due to its specific terrain and complex PBL meteorology. The modeling results in the eastern plain stations (Cangzhou, etc.) of the 3JNS were better than the west (Zhangjiakou, Xingtai, etc.) as mentioned in the section 3.1.

Figure 6 displays the hourly variations of aera mean $PM_{2.5}$, wind speed at 10 m, the PBLH, and vertical diffusivity at level 8 (Table 3) of the four PBL schemes during the haze episode (total duration: 120 hours). The YSU scheme simulated the lowest concentration, followed by the Boulac and MYJ schemes, and the ACM2 scheme simulating the highest concentration. It can be seen from this figure that the $PM_{2.5}$ concentrations simulated using the YSU, MYJ and Boulac schemes all possessed good inverse relationships with wind speed at 10 m, the PBLH, and vertical diffusivity. After sunrise, with the strengthening of solar radiation, the turbulent diffusivity within the PBL continued to enhance, the PBLH and wind speed also increased, and all three variables reached their maximum at about 07:00 UTC (local 3 o'clock in the afternoon). After then, all three variables weakened with solar radiation and remained stable at night (after sunset). For the reasons outlined above, the concentration of simulated $PM_{2.5}$ during daytime was lower than at night. Owing to the lack of turbulent diffusivity, the modeled $PM_{2.5}$ using the ACM2 scheme was not only substantially higher than that of the other three schemes, but also produced an opposite change trend during the daytime compared with the other three schemes. In summary, in the model, the effects of vertical diffusion on the hourly change trend of $PM_{2.5}$ are much more important compared with the effects on daily averaged $PM_{2.5}$.

3.3 Vertical profiles of PM2.5 and meteorology within the PBL

The structure of PBL vertical meteorology is very important to particle diffusion, vertical and horizontal transportation, and thus the simulation of $PM_{2.5}$. Unfortunately, air sounding observations are only carried out by the CMA at 00:00 UTC (early moring, local time) and 12:00 UTC (nightfall), meaning observational data in terms of the vertical profiles of meteorological parameters during local daytime—local noon (06:00 UTC) especially—are not available and therefore cannot be used for model validation in China at present. Accordingly, Figure 7 only compares the modeled $PM_{2.5}$ concentration, wind speed and vertical diffusion using the four PBL schemes. Each value of the profile was first avereraged over the stations in 3JNS, and then averaged over the duration of the haze process (120 hours). The model levels and their corresponding heights are displayed in Table 3. It can be seen from Figure 7 that the differences among the profiles of the YSU, MYJ and Boulac schemes were small, ranging from 160 μg m^{-3} to 165 μg m^{-3}. The $PM_{2.5}$ using the ACM2 scheme produced higher accumulation at ground level, and its rate of vertical decrease was the largest. The differences between ACM2 and the three other PBL schemes were obvious. The $PM_{2.5}$ values simulated using the ACM2 scheme were much higher than those of the three other PBL schemes under levels 10–11 (300–400 m), but much smaller above this height. The discrepancies in the $PM_{2.5}$ concentrations and PBL variables among different PBL schemes were mainly apparent beneath level 11 (height of approximately 402 m). Just under this height local diffusion was strongest, indicating that local vertical diffusion occurring mainly from 100 m to 400 m, and heights below 400 m, were important for the $PM_{2.5}$ simulation. The results also showed that the surface $PM_{2.5}$ concentration was affected by the wind speed and diffusion collectively throughout the whole PBL (especially under 400 m), rather the surface only.

3.4 Diurnal variation of surface $PM_{2.5}$, emissions and vertical diffusion

It can be seen from the discussion on Figure 6 in section 3.2 that the modeling $PM_{2.5}$ using ACM2 produced an opposite change trend during daytime compared with the three other PBL schemes, which was due to there being no claculation of local particle diffusion in the ACM2 scheme. The diurnal variation of vertical diffusion and $PM_{2.5}$ concentration of haze and clean days using the four PBL schemes is displayed in Figures 8c–8f, along with the diurnal variation of emissions in Figures 8a and 8b. These figures show exactly how diffusion affected the $PM_{2.5}$ trend during the course of one day, from 00:00 UTC to 23:00 UTC. The values of $PM_{2.5}$ and diffusion were both averaged over 48 $PM_{2.5}$ stations in the 3JNS, and each hour was also averaged during haze (Feburary 21 to 25) and clean periods (Feburary 3 to 5) seperately. Most stations' daily averaged PM2.5 of observations were above 200 μg m^{-3} in the "haze" while under the 50μg m^{-3} in the "clean" days. The diurnal variation produced by the four PBL schemes was exactly the same as shown in Figure 6. The diurnal change trend of $PM_{2.5}$ was largely a synthesis of the change in emissions and vertical diffusion. When diffusion was absent, as in the ACM2 scheme, the variation of $PM_{2.5}$ was extremely close to that of emissions. As such, the concentration of $PM_{2.5}$ was much higher than observed throughout the entire day, but especially during local daytime from 00:00 to 11:00 UTC, both for haze days (Figure 8e) and clean days (Figure 8f). This indicates that not claculating local particle diffusion during the daytime may result in higher surface $PM_{2.5}$ throughout the entire day, since it prevents particles from moving upward and therefore results in efficient horizontal transport. The $PM_{2.5}$ simulated using the YSU, MYJ and Boulac schemes was obviously lower than observed during daytime, and their dirunal variation of $PM_{2.5}$ disagreed with, and even contrasted with the ovservation especially for haze days. Comparing this result with that of the ACM2 sheme, it can be concluded that the three PBL schemes overestimated the vertical diffusion process in the 3JNS region, leading to lower simulated surface $PM_{2.5}$ and negative errors during daytime, particularly when severe haze occurred, which is in agreement with the data shown in Table 2.

There are two reasons for this strong diffusion and lower $PM_{2.5}$ during daytime. The direct radiative feedback of aerosols may lead to weaker diffusion, a more stable atmosphere, and higher surface $PM_{2.5}$ when the $PM_{2.5}$ concentration is higher than a certain threshold [26, 46]. However, this feedback was not calculated in the present study. In addition, it was the calculation methods with respect to vertical diffusion by three of the PBL schemes that led to stronger particle diffusion and lower surface $PM_{2.5}$ than was actually the case in the real atmosphere. Turbulent diffusion is a major factor affecting the diurnal variation of PM2.5, but not the only reason determining concentrations.

It should be noted that the different representations of vertical diffusion in these PBL schemes might have different impacts on $PM_{2.5}$ simulation under different conditions of atmospheric stability in different regions. So here, the same five stations mentioned above were picked up again to illustrate the modeling result of diurnal variations over different topography (Figure 9). For the small difference of vertical diffusivity between haze and clean period at the five stations, the figures of diffusion were ignored here. Though there's no significant pattern in the diurnal variations of observation, this figure also indicated that the simulated diurnal variations of PM2.5 of specific stations weren't as well as daily averaged variations in Figure 5. Despite this, the modeled trends of Taiyuan and the eastern city Cangzhou were relatively good. By the influence of Taihang Mountains, Xingtai simulated lower PM2.5 in haze days and higher PM2.5 in clean days compared with observations. When the model performed well in haze with high PM2.5 concentrations (Taiyuan and Cangzhou), it simulated apparently higher PM2.5 in the clean days with lower PM2.5 concentrations, and vice versa for Zhangjiakou. It seems to be that the little difference of diffusivity calculation between haze and clean days by all the PBL schemes calculation might lead to this interesting phenomenon, which is probably the main way to improve PM2.5 forecasting in complex topography.

4 Conclusion

To explore the impacts of different PBL schemes on $PM_{2.5}$ simulation, four PBL schemes (YSU, MYJ, ACM2, Boulac) were applied in the WRF-Chem model to simulate haze episodes that occurred in the Jing-Jin-Ji region and its surroundings of China. The research area is abbreviated to 3JNS in this paper.

The results of the four PBL schemes in simulating the $PM_{2.5}$ concentration over 3JNS showed that all four schemes performed similarly with respect to the $PM_{2.5}$ trend during a month that included haze episodes. However, among them, the Boulac scheme produced the least bias for haze period, followed by the YSU and MYJ scheme, and these three schemes showed negligible difference in simulating the $PM_{2.5}$ concentration. Owing to the lack of diffusivity in the chemistry module, the $PM_{2.5}$ concentration simulated using the ACM2 scheme was higher than observed, and higher than that simulated in the three other schemes. All four PBL schemes simulated similar daily trends in $PM_{2.5}$ concentration, which was in agreement with the observation and possessed a good inverse relationship with the PBLH and wind speed—better than with vertical diffusion. All the PBL schemes behaves diversely in different terrains. On the whole, eastern plain cities such as Cangzhou and Chengde produced better simulation results than the western cities such as Zhangjiakou and Baoding which near mountains; the cities under the eastern root of Taihang Mountain produced the worst results in simulating high PM2.5 and wind speed; the modeling results of plain cities were better than the cities under the mountain (e.g. Beijing under the Yan Mountain). Study results showd that all the four PBL schemes hadn't enough ability in distinguishing the local PBL meteorologies including daytime diffusion and wind speed between haze and clean days in the complex topography area in China, which may be regarded as an important direction for the improving of PM2.5 simulation. The heights under or near the 400 m were found to be very important for $PM_{2.5}$ simulation. The $PM_{2.5}$ concentration simulated using the ACM2 scheme produced higher accumulation at ground level, and its rate of vertical decrease was the largest among all the schemes. ACM2 was used as a reference scheme for comparison with the three other schemes, to describe the diurnal impacts of vertical diffusion on $PM_{2.5}$ simulation. The effects of vertical diffusion on the hourly change trend of $PM_{2.5}$ simulation were far more important than those on the simulation of daily averaged $PM_{2.5}$. Diurnal variation of $PM_{2.5}$ was largely a synthesis of the change in emissions and vertical diffusion. If lacking diffusivity, as with the ACM2 scheme, the diurnal variation of $PM_{2.5}$ and emissions were similar and the $PM_{2.5}$ concentration for the whole day was overestimated. Compared with the ACM2 scheme, the three other PBL schemes overestimated the vertical diffusion process in the 3JNS, leading to a lower simulation of surface $PM_{2.5}$ and negative errors during daytime—partically when severe haze occurred. In addition, the small gap of diffusivity between haze and clean days by PBL schemes may lead to the errors in simulating PM2.5 concentrations.

Though the differences in $PM_{2.5}$ concentration among the PBL scehmes were very small, the exact reasons related to these differences were not discussed in this study. The reasons for the poor reflection of diurnal variation in the PBL schemes, resulting in $PM_{2.5}$ errors in numerical models, need to be studied in detail, and then adjustments made to improve results for different regions.

Conflict of Interest

The authors declare that there is no conflict of interest regarding the publication of this article.

Acknowledgments:

This work is supported by National Natural Scientific Foundation of China (41275007), 973 Program of Ministry of Science and Technology of China (2014CB441201), National Science and Technology Project of China (2014BAC22B04).

References

[1] Y. Ding and Y. Liu, "Analysis of long-term variations of fog and haze in China in recent 50 years and their relations with atmospheric humidity," *Science China Earth Sciences*, vol. 57, no. 1, pp. 36-46, 2013.

[2] M. Li and L. Zhang, "Haze in China: current and future challenges," *Environmental pollution*, vol. 189, no., pp. 85-6, 2014.

[3] H. Che, X. Zhang, Y. Li, et al., "Haze trends over the capital cities of 31 provinces in China, 1981–2005," *Theoretical and Applied Climatology*, vol. 97, no. 3-4, pp. 235-42, 2008.

[4] P. Zhao, X. Zhang, X. Xu, et al., "Long-term visibility trends and characteristics in the region of Beijing, Tianjin, and Hebei, China," *Atmospheric Research*, vol. 101, no. 3, pp. 711-8, 2011.

[5] F. Chai, J. Gao, Z. Chen, et al., "Spatial and temporal variation of particulate matter and gaseous pollutants in 26 cities in China," *Journal of Environmental Sciences*, vol. 26, no. 1, pp. 75-82, 2014.

[6] X. Y. Zhang, Y. Q. Wang, T. Niu, et al., "Atmospheric aerosol compositions in China: spatial/temporal variability, chemical signature, regional haze distribution and comparisons with global aerosols," *Atmospheric Chemistry and Physics*, vol. 12, no. 2, pp. 779-99, 2012.

[7] Q. Zhang, Z. Shen, J. Cao, et al., "Variations in PM2.5, TSP, BC, and trace gases (NO2, SO2, and O3) between haze and non-haze episodes in winter over Xi'an, China," *Atmospheric Environment*, vol. 112, no., pp. 64-71, 2015.

[8] X. Fu, S. X. Wang, Z. Cheng, et al., "Source, transport and impacts of a heavy dust event in the Yangtze River Delta, China, in 2011," *Atmos Chem Phys*, vol. 14, no. 3, pp. 1239-54, 2014.

[9] X. Wang, J. Chen, J. Sun, et al., "Severe haze episodes and seriously polluted fog water in Ji'nan, China," *The Science of the total environment*, vol. 493, no., pp. 133-7, 2014.

[10] P. S. Zhao, F. Dong, D. He, et al., "Characteristics of concentrations and chemical compositions for PM2.5 in the region of Beijing, Tianjin, and Hebei, China," *Atmos Chem Phys*, vol. 13, no. 9, pp. 4631-44, 2013.

[11] M. Tao, L. Chen, Z. Wang, et al., "A study of urban pollution and haze clouds over northern China during the dusty season based on satellite and surface observations," *Atmospheric Environment*, vol. 82, no. 0, pp. 183-92, 2014.

[12] H. Wang, S.-C. Tan, Y. Wang, et al., "A multisource observation study of the severe prolonged regional haze episode over eastern China in January 2013," *Atmospheric Environment*, vol. 89, no. 0, pp. 807-15, 2014.

[13] Q. Zhang, D. G. Streets, G. R. Carmichael, et al., "Asian missions in 2006 for the NASA INTEX-B mission," *Atmos. Chem. Phys.*,vol. 9, no., pp. 5131-5153, 2009.

[14] S. Wang, D. G. Streets, Q. Zhang, et al., "Satellite detection and model verification of NOxemissions from power plants in Northern China," *Environmental Research Letters*, vol. 5, no. 4, pp. 044007, 2010.

[15] M. Li, Q. Zhang, D. G. Streets, et al., "Mapping Asian anthropogenic emissions of non-methane volatile organic compounds to multiple chemical mechanisms," *Atmospheric Chemistry and Physics*, vol. 14, no. 11, pp. 5617-38, 2014.

[16] Z. Wang, J. Li, Z. Wang, et al., "Modeling study of regional severe hazes over mid-eastern China in January 2013 and its implications on pollution prevention and control," *Science China Earth Sciences*, vol. 57, no. 1, pp. 3-13, 2013.

[17] Y. Gao, M. Zhang, Z. Liu, et al., "Modeling the feedback between aerosol and meteorological variables in the atmospheric

boundary layer during a severe fog–haze event over the North China Plain," *Atmospheric Chemistry and Physics*, vol. 15, no. 8, pp. 4279-95, 2015.

[18] X. Tie, Q. Zhang, H. He, et al., "A budget analysis of the formation of haze in Beijing," *Atmospheric Environment*, vol. 100, no., pp. 25-36, 2015.

[19] Q. Zhang, C. Zhao, X. Tie, et al., "Characterizations of aerosols over the Beijing region: A case study of aircraft measurements," *Atmospheric Environment*, vol. 40, no. 24, pp. 4513-27, 2006.

[20] G. J. Zheng, F. K. Duan, H. Su, et al., "Exploring the severe winter haze in Beijing: the impact of synoptic weather, regional transport and heterogeneous reactions," *Atmospheric Chemistry and Physics*, vol. 15, no. 6, pp. 2969-83, 2015.

[21] J. Quan, X. Tie, Q. Zhang, et al., "Characteristics of heavy aerosol pollution during the 2012–2013 winter in Beijing, China," *Atmospheric Environment*, vol. 88, no., pp. 83-9, 2014.

[22] C. M. Gan, Y. Wu, B. L. Madhavan, et al., "Application of active optical sensors to probe the vertical structure of the urban boundary layer and assess anomalies in air quality model PM2.5 forecasts," *Atmospheric Environment*, vol. 45, no. 37, pp. 6613-21, 2011.

[23] Q. Zhang, J. Quan, X. Tie, et al., "Effects of meteorology and secondary particle formation on visibility during heavy haze events in Beijing, China," *The Science of the total environment*, vol. 502, no., pp. 578-84, 2015.

[24] H. He, X. Tie, Q. Zhang, et al., "Analysis of the causes of heavy aerosol pollution in Beijing, China: A case study with the WRF-Chem model," *Particuology*, vol. 20, no. 0, pp. 32-40, 2015.

[25] J. Quan, Y. Gao, Q. Zhang, et al., "Evolution of planetary boundary layer under different weather conditions, and its impact on aerosol concentrations," *Particuology*, vol. 11, no. 1, pp. 34-40, 2013.

[26] H. Wang, M. Xue, X. Y. Zhang, et al., "Mesoscale modeling study of the interactions between aerosols and PBL meteorology during a haze episode in Jing–Jin–Ji (China) and its nearby surrounding region – Part 1: Aerosol distributions and meteorological features," *Atmospheric Chemistry and Physics*, vol. 15, no. 6, pp. 3257-75, 2015.

[27] X. M. Hu, P. M. Klein and M. Xue, "Evaluation of the updated YSU planetary boundary layer scheme within WRF for wind resource and air quality assessments," *Journal of Geophysical Research: Atmospheres*, vol. 118, no. 18, pp. 10,490-10,505, 2013.

[28] X. M. Hu, J. W. Nielsen-Gammon and F. Zhang, "Evaluation of Three Planetary Boundary Layer Schemes in the WRF Model," *Journal of Applied Meteorology and Climatology*, vol. 49, no. 9, pp. 1831-44, 2010.

[29] X. M. Hu, F. Zhang and J. W. Nielsen-Gammon, "Ensemble-based simultaneous state and parameter estimation for treatment of mesoscale model error: A real-data study," *Geophysical Research Letters*, vol. 37, no. 8, pp. n/a-n/a, 2010.

[30] X. M. Hu, P. M. Klein, M. Xue, et al., "Impact of Low-Level Jets on the Nocturnal Urban Heat Island Intensity in Oklahoma City," *Journal of Applied Meteorology and Climatology*, vol. 52, no. 8, pp. 1779-802, 2013.

[31] X. M. Hu, P. M. Klein, M. Xue, et al., "Impact of the vertical mixing induced by low-level jets on boundary layer ozone concentration," *Atmospheric Environment*, vol. 70, no., pp. 123-30, 2013.

[32] X. M. Hu, D. C. Doughty, K. J. Sanchez, et al., "Ozone variability in the atmospheric boundary layer in Maryland and its

implications for vertical transport model," *Atmospheric Environment*, vol. 46, no., pp. 354-64, 2012.

[33] G. A. Grell, S. E. Peckham, R. Schmitz, et al., "Fully coupled “online” chemistry within the WRF model," *Atmospheric Environment*, vol. 39, no. 37, pp. 6957-75, 2005.

[34] J. D. Fast, W. I. Gustafson, R. C. Easter, et al., "Evolution of ozone, particulates, and aerosol direct radiative forcing in the vicinity of Houston using a fully coupled meteorology-chemistry-aerosol model," *Journal of Geophysical Research: Atmospheres*, vol. 111, no. D21, pp. D21305, 2006.

[35] R. A. Zaveri and L. K. Peters, "A new lumped structure photochemical mechanism for large-scale applications," *Journal of Geophysical Research*, vol. 104, no. D23, pp. 30387, 1999.

[36] Oliver Wild, Xin Zhu and Michael J. Prather. "Fast-J: Accurate simulation of in- and below-colud photolysis in tropospheric chemical models," *Journal of Atmospheric Chemistry*, vol. 37, no., pp. 245-282, 2000.

[37] E. J. Mlawer, S. J. Taubman, P. D. Brown, et al., "Radiative transfer for inhomogeneous atmospheres: RRTM, a validated correlated-k model for the longwave," *Journal of Geophysical Research*, vol. 102, no. D14, pp. 16663, 1997.

[38] Y. L. Lin, R. D. Farley and H. D. Orville, "Bulk Parameterization of the Snow Field in a Cloud Model," *Journal of Climate and Applied Meteorology*, vol. 22, no. 6, pp. 1065-92, 1983.

[39] S. W. Wang, Q. Zhang, D. G. Streets, et al., "Growth in NOx emissions from power plants in China: bottom-up estimates and satellite observations," *Atmospheric Chemistry and Physics*, vol. 12, no. 10, pp. 4429-47, 2012.

[40] B. Xie, J. C. H. Fung, A. Chan, et al., "Evaluation of nonlocal and local planetary boundary layer schemes in the WRF model," *Journal of Geophysical Research: Atmospheres*, vol. 117, no. D12, pp. D12103, 2012.

[41] Songyou Hong and Ying Noh. "A new vertical diffusion package with an explicit treatment of entrainment processes," *Monthly Weather Review*, vol. 134, no., pp. 2318-2341, 2006.

[42] Songyou Hong and Hualu Pan. "Nonlocal Boundary Layer Vertical diffusion in a medium-range forecast model," *Monthly Weather Review*, vol. 124, no., pp. 2322-2339, 1996.

[43] Zavisa I. Janjic. "The step-mountain eta coordinate model: further developments of the convection, viscous subpayer, and turbulence closure schemes," *Monthly Weather Review*, vol. 122, no., pp. 927-945, 1994.

[44] J. E. Pleim, "A Combined Local and Nonlocal Closure Model for the Atmospheric Boundary Layer. Part I: Model Description and Testing," *Journal of Applied Meteorology and Climatology*, vol. 46, no. 9, pp. 1383-95, 2007.

[45] P. Bougeault and P. Lacarrère, "Parameterization of orography-induced turbulence in a mesobeta-scale model," *Monthly Weather Review*, vol. 117, no., pp. 1872-1890, 1989.

[46] H. Wang, G. Y. Shi, X. Y. Zhang, et al., "Mesoscale modelling study of the interactions between aerosols and PBL meteorology during a haze episode in China Jing–Jin–Ji and its near surrounding region – Part 2: Aerosols' radiative feedback effects," *Atmospheric Chemistry and Physics*, vol. 15, no. 6, pp. 3277-87, 2015.

Table 1. Main physical schemes used in WRF-Chem.

Physical process	Physics option
Shortwave radiation	Goddard
Longwave radiation	RRTM
Microphysics	Lin
Cumulus parameterization	New Grell scheme
Planetary boundary layer	YSU MYJ ACM2 Boulac
Surface layer	Revised MM5 Monin–Obukhov for YSU, ACM2, and Boulac Monin–Obukhov for MYJ
Land surface	Unified Noah Land-Surface Model

Table 2. Comparisons of statistical indicators of $PM_{2.5}$
(Haze: Feb 21 to 25 – daytime, 00:00–11:00 UTC; night, 12:00–24:00 UTC. Clean days: Feb 3 to 5. Unit: μg m^{-3})

	YSU		MYJ		ACM2		Boulac	
	MB	NMB	MB	NMB	MB	NMB	MB	NMB
Whole month	17.7	15.9%	24.5	22.0%	54.9	49.2%	21.2	19.0%
Haze episode	−2.5	-1.4%	5.4	3.0%	47.3	26.7%	0.13	0.5%
Haze daytime	−11.8	-6.8%	−1.8	−1.0%	58.6	33.6%	−8.1	−4.6%
Haze night	7.2	4.0%	13.2	7.3%	35.3	19.6%	8.9	4.9%
	NME	RMSE	NME	RMSE	NME	RMSE	NME	RMSE
Whole month	49.8%	104.0	52.5%	106.0	68.7%	119.3	49.8%	103.8
Haze episode	31.2%	76.6	31.4%	75.4	40.9%	92.6	31.2%	74.6
Haze daytime	31.0%	76.6	30.6%	73.9	45.2%	98.7	30.6%	75.8
Haze night	31.4%	76.6	32.1%	76.9	36.4%	85.6	31.8%	77.5
Haze / clean	174.4 / 64.9		182.4 / 70.4				177.1 / 69.2	
	Haze	Clean	Haze	Clean			Haze	Clean
Maximum	217.8	22.2	220.5	30.4			220.6	27.6
Minimum	98.1	24.4	100.2	26.7			105.8	28.5

Table 3. Model levels and their corresponding heights.

Model Level	1	2	3	4	5	6	7	8	9	10	11	12	13	14	15	16	17
Geopotential height (m)	0	15	30	45	61	91	137	175	222	315	402	586	767	943	1132	1307	1496

Figure Captions:

Figure 1. Nested modeling domains (left), the distribution of observation sites within domain 2 (right: filled circles, $PM_{2.5}$ observation sites; open circles, surface meteorological sites; open triangles: upper-air meteorological stations; the dashed-line square area represents the research area (3JNS) referred to.) and the topography of the research area (bottom).

Figure 2. Mean simulated (shaded) and observed (dotted) $PM_{2.5}$ values during the haze period (Feb 21 to 25).

Figure 3. Simulated and observed hourly $PM_{2.5}$ concentration at 10 sites in Feburary 2014.

Figure 4. Variation of the daily averaged $PM_{2.5}$ concentration, wind speed (near-surface), PBLH, and vertical diffusivity of the area mean in Feburary.

Figure 5. Variation of the daily averaged $PM_{2.5}$ concentration and wind speed (near-surface) at 5 sites of different terrain in Feburary

Figure 6. Variation of the area-averaged $PM_{2.5}$ concentration, wind speed at 10m, PBLH, and vertical diffusivity during the haze process.

Figure 7. Vertical profiles of the $PM_{2.5}$ concentration, wind speed, and vertical diffusivity.

Figure 8. Diurnal variation of emissions, $PM_{2.5}$, and vertical diffusion.

Figure 9. Diurnal variation of $PM_{2.5}$ in polluted and clean process at 5 sites of different terrain.

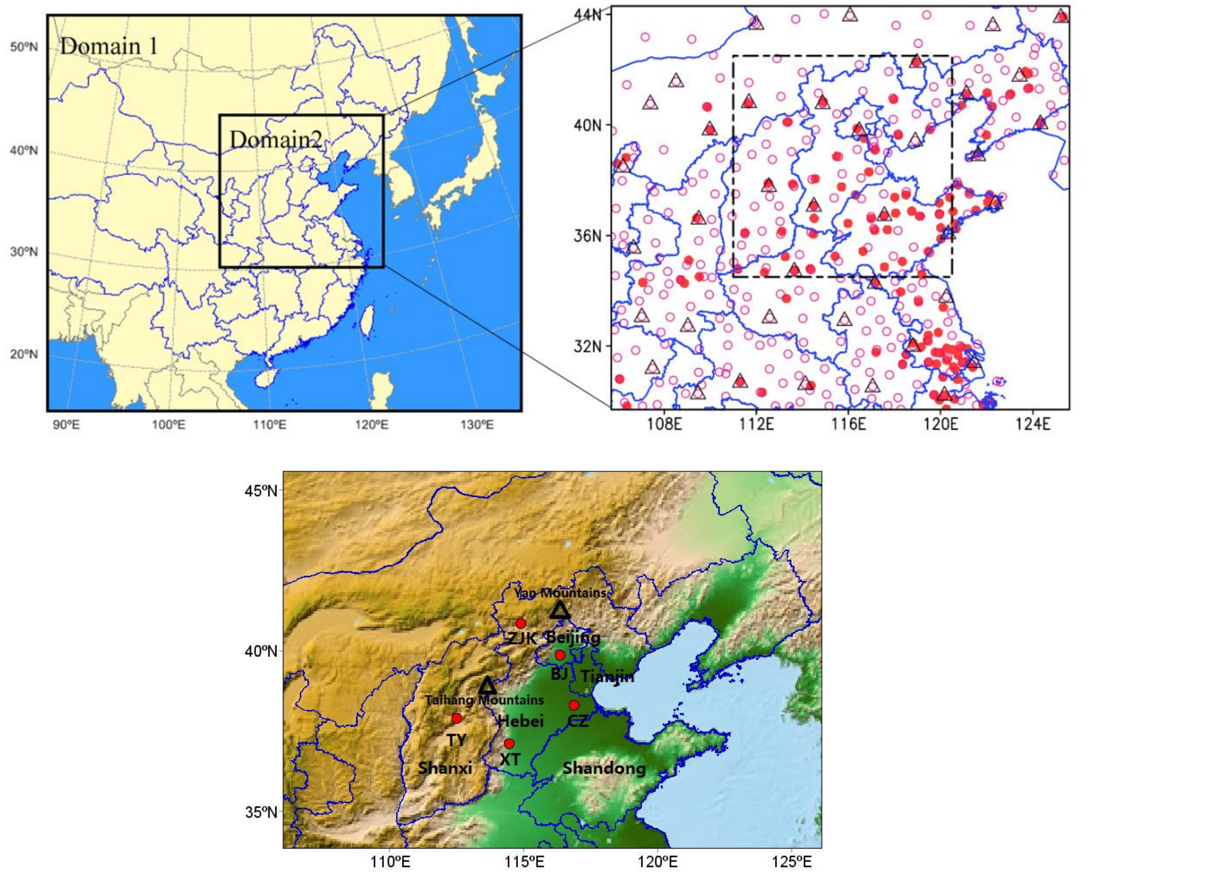

Figure 1. Nested modeling domains (left), the distribution of observation sites within domain 2 (right: filled circles, $PM_{2.5}$ observation sites; open circles, surface meteorological sites; open triangles: upper-air meteorological stations; the dashed-line square area represents the research area (3JNS) referred to.) and the topography of the research area (bottom).

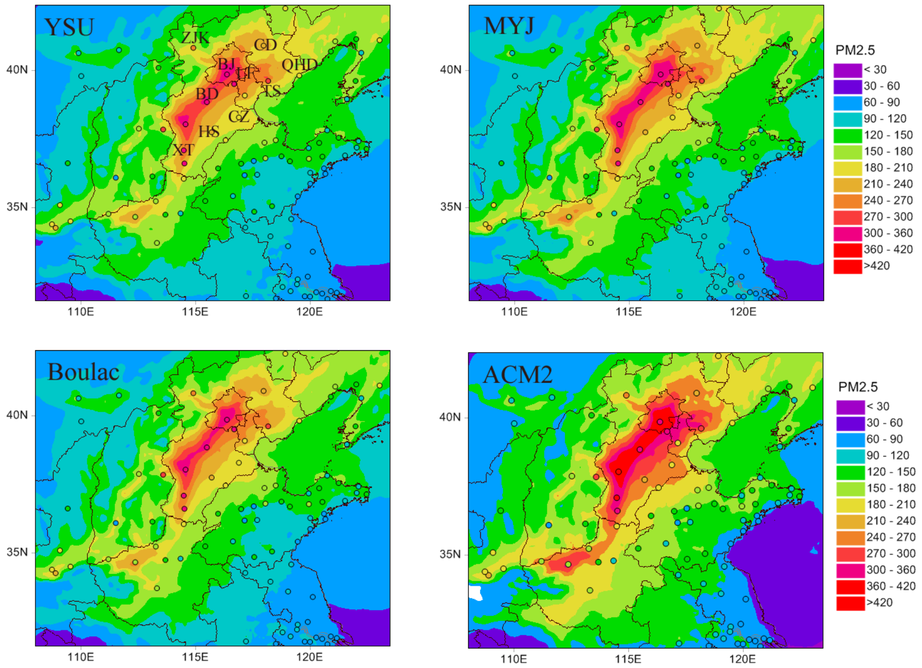

Figure 2. Mean simulated (shaded) and observed (dotted) $PM_{2.5}$ values during the haze period (Feb 21 to 25).

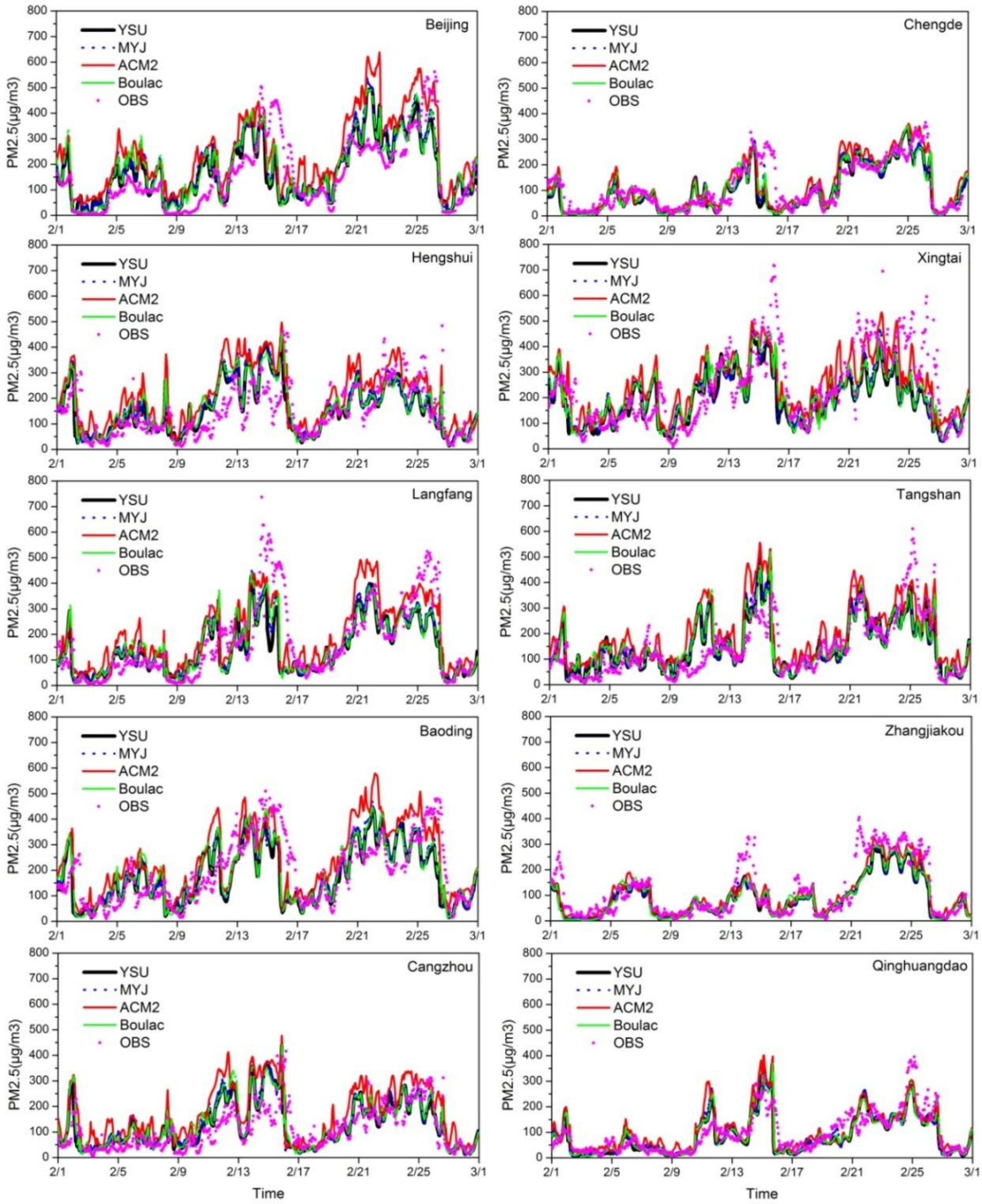

Figure 3. Simulated and observed hourly $PM_{2.5}$ concentration at 10 sites in Feburary 2014.

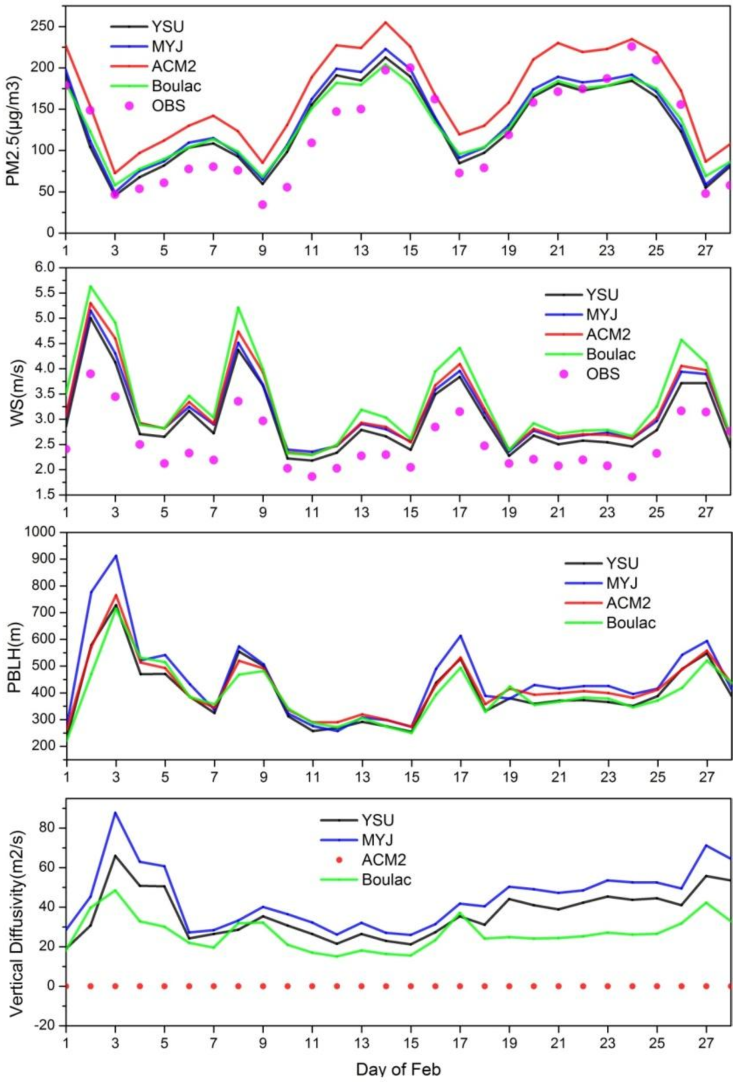

Figure 4. Variation of the daily averaged $PM_{2.5}$ concentration, wind speed (near-surface), PBLH, and vertical diffusivity of the area mean in Feburary.

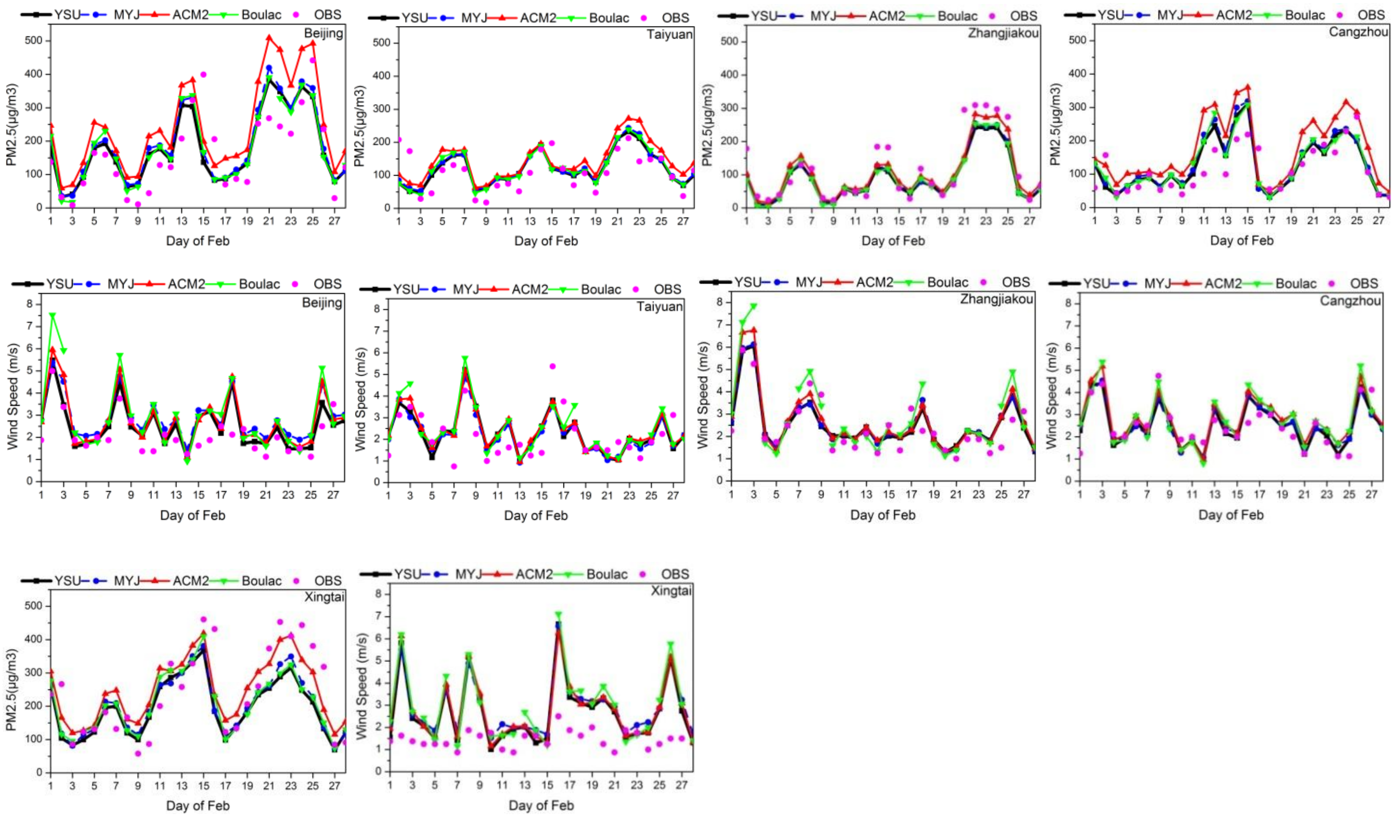

Fig 5. Variation of the daily averaged $PM_{2.5}$ concentration and wind speed (near-surface) at 5 sites of different terrain in Feburary

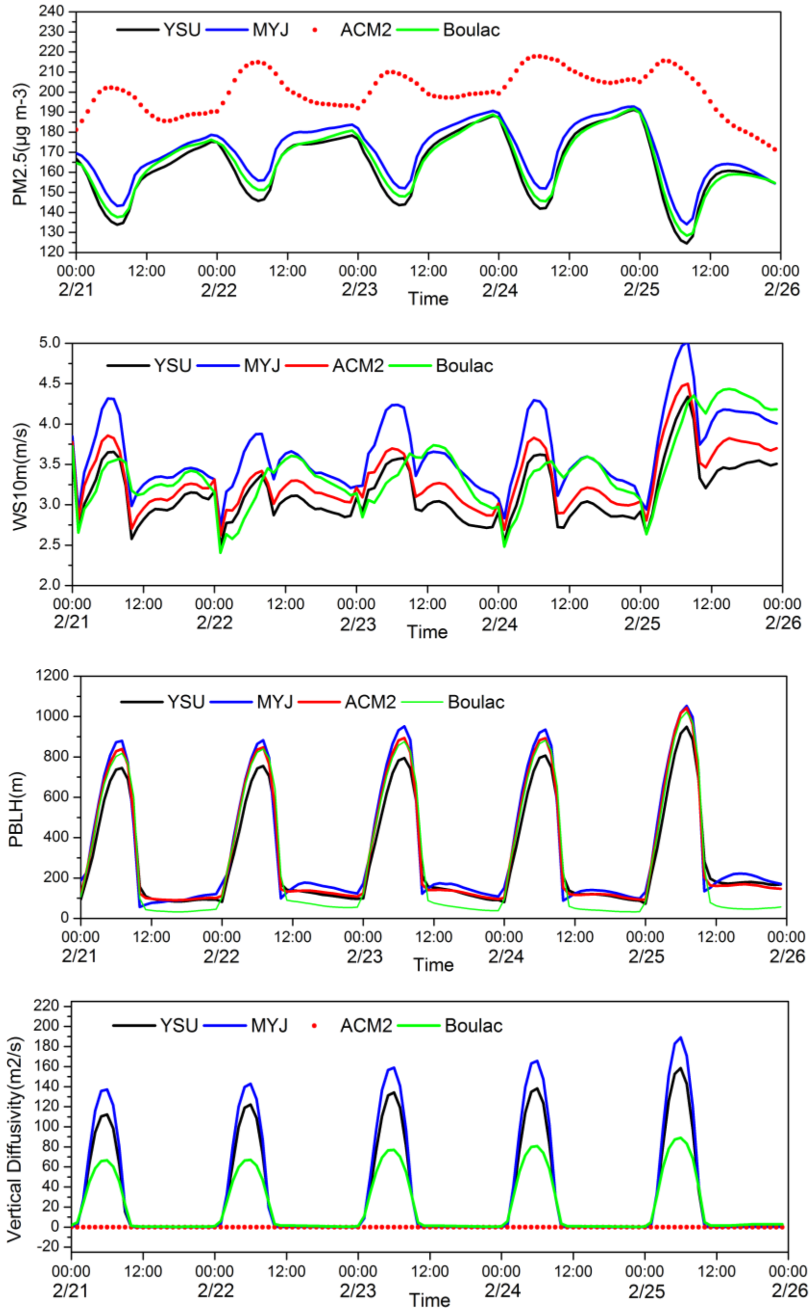

Figure 6. Variation of the area-averaged $PM_{2.5}$ concentration, wind speed at 10m, PBLH, and vertical diffusivity during the haze process.

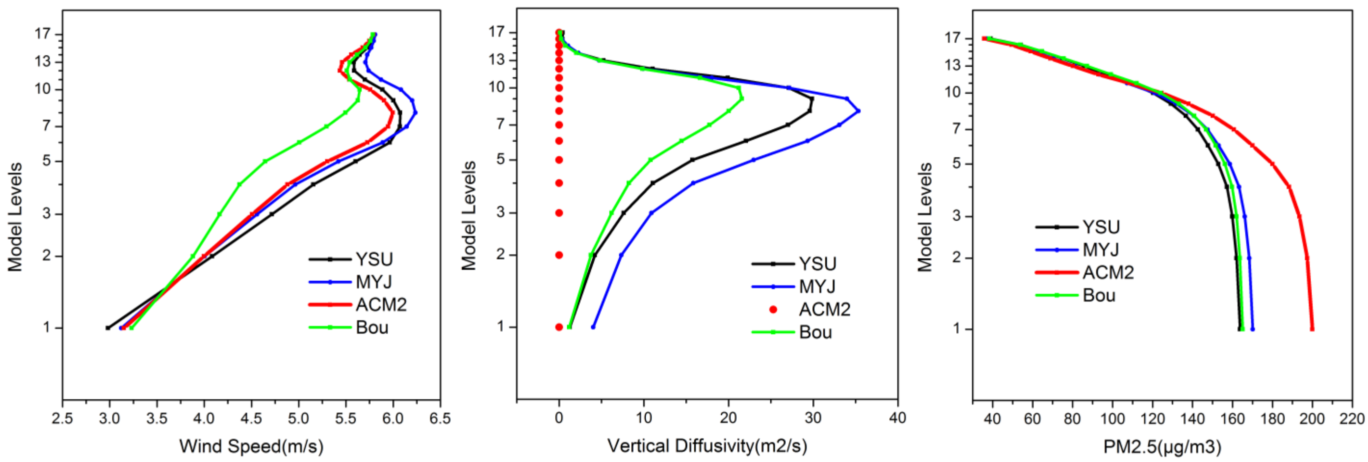

Figure 7. Vertical profiles of the $PM_{2.5}$ concentration, wind speed, and vertical diffusivity.

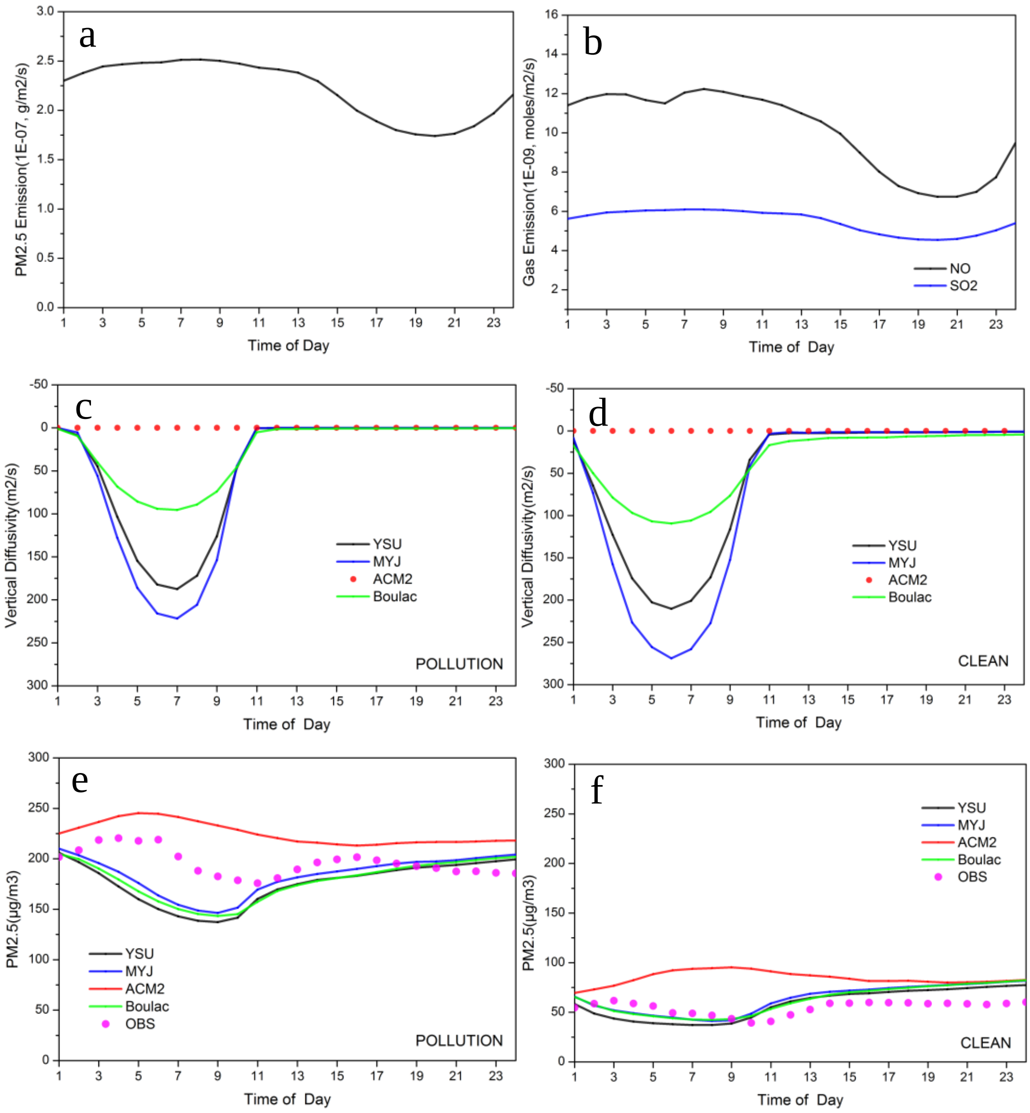

Figure 8. Diurnal variation of emissions, $PM_{2.5}$, and vertical diffusion

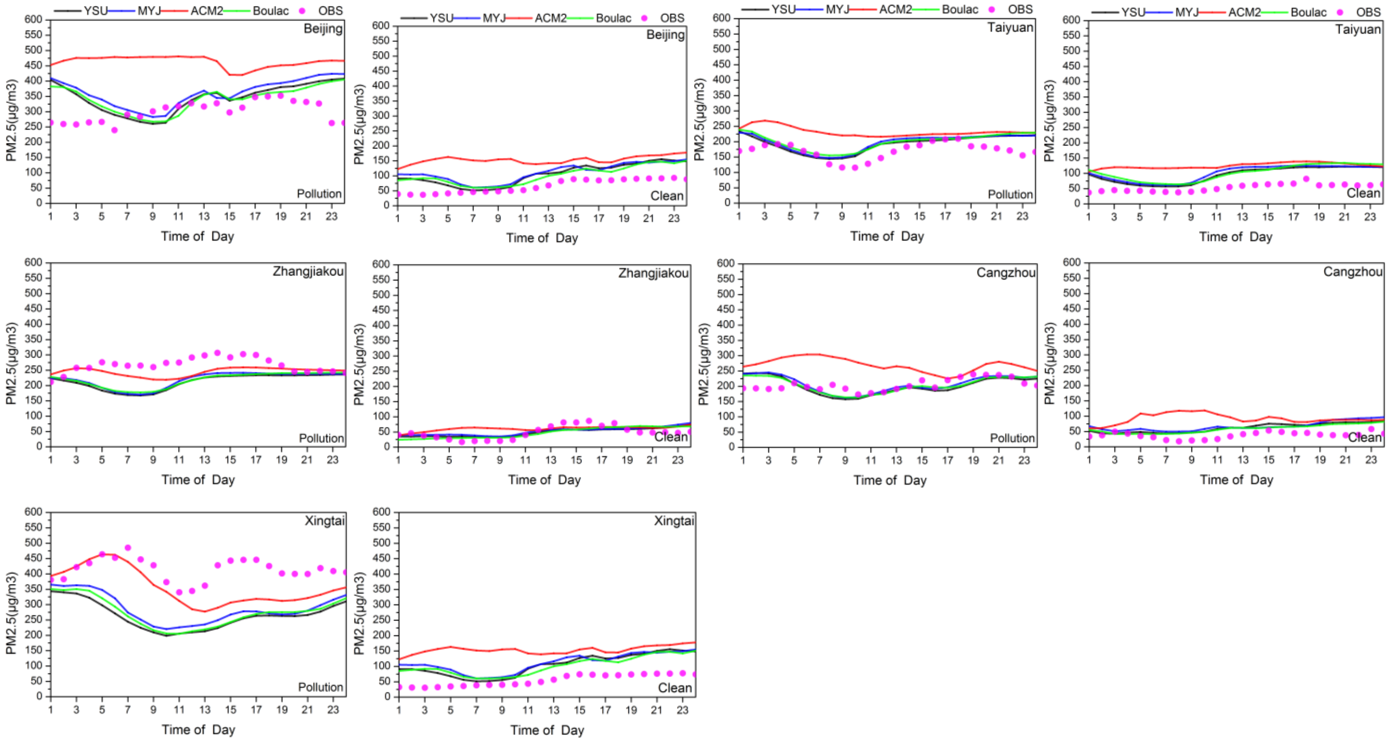

Figure 9. Diurnal variation of $PM_{2.5}$ in polluted and clean process at 5 sites of different terrain.